Nuclear Microscopy: A Tool for Imaging Elemental Distribution and Percutaneous Absorption In Vivo

ANA VERÍSSIMO,[1] LUÍS C. ALVES,[1] PAULO FILIPE,[2] JOÃO N. SILVA,[2] RAQUEL SILVA,[2] MARIA DOLORES YNSA,[3,4] ETIENNE GONTIER,[3] PHILIPPE MORETTO,[3] JAN PALLON,[5] AND TERESA PINHEIRO[1]*

[1]*LFI, Instituto Tecnológico e Nuclear, Sacavém and Centro de Física Nuclear, Universidade de Lisboa, Lisboa, Portugal*
[2]*Clínica Dermatológica Universitária, Hospital de Santa Maria, and Faculdade de Medicina de Lisboa, Lisboa, Portugal*
[3]*CENBG-IN2P3/CNRS, Gradignan, France*
[4]*Centro de Microanálisis de Materiales, Universidad Autónoma de Madrid, Madrid, Spain*
[5]*Physics Department, Lund Institute of Technology, Lund University, Lund, Sweden*

KEY WORDS human skin; metals; X-ray microscopy; STIM; PIXE

ABSTRACT Nuclear microscopy is a technique based on a focused beam of accelerated particles that has the ability of imaging the morphology of the tissue in vivo and of producing the correspondent elemental maps, whether in major, minor, or trace concentrations. These characteristics constitute a strong advantage in studying the morphology of human skin, its elemental distributions and the permeation mechanisms of chemical compounds. In this study, nuclear microscopy techniques such as scanning transmission ion microscopy and particle induced X-ray emission were applied simultaneously, to cryopreserved human skin samples with the purpose of obtaining high-resolution images of cells and tissue morphology. In addition, quantitative elemental profiling and mapping of phosphorus, calcium, chlorine, and potassium in skin cross-sections were obtained. This procedure accurately distinguishes the epidermal strata and dermis by overlapping in real time the elemental information with density images obtained from the transmitted beam. A validation procedure for elemental distributions in human skin based on differential density of epidermal strata and dermis was established. As demonstrated, this procedure can be used in future studies as a tool for the in vivo examination of trans-epidermal and -dermal delivery of products. *Microsc. Res. Tech. 70:000–000, 2007.*

INTRODUCTION

Human skin provides an excellent barrier to avoid outward percutaneous water loss and inward penetration of external agents, either biological or chemical. However, the persistent long-term contact of the skin to certain cosmetic, household, or pharmacological products may bias skin function, as corneocyte layers of skin are continuously affected (Fluhr et al., 2005; Nielsen et al., 2000; Tsuji et al., 2006). The influence of dermatological afflictions on the quality of life has recently raised the concern of both clinical practitioners and associations of consumer's protection. Many research efforts have been invested in studying the skin physiology and the mechanisms of skin permeability to inorganic or metal compounds. Considerable knowledge has been gathered despite the broad margins of variability observed for skin as a target organ, although the mechanisms by which permeable compounds influence skin metabolism and barrier function are still not fully clarified. Numerous studies on this matter have been conducted over the past 25 years, some associated with the purpose of using the skin as an alternative route for systemic administration of active drugs (Barry, 2001; Forslind et al., 1997; Hadgraft, 2004; Hostynek, 2003; Pallon et al., 2006; Pechtold et al., 2001; Thomas and Finnin, 2004).

Several methodologies have been developed to quantify the percutaneous absorption of products, either in vivo or in vitro. The most common in vivo procedure is to estimate the diffusion of topically applied products by tape stripping. Nevertheless, this method is limited to the upper skin layer, the *stratum corneum*, and the results can be influenced by the anatomic site, tape application pressure, duration, and removal (Löffer et al., 2004; Van der Molen et al., 1997). Eventually, the procedure can induce irritant dermatitis (Fluhr et al., 2005). As such, this method is unable to give a complete diffusion profile of the skin as a whole or a straightforward interpretation of its results. Alternative procedures such as in vitro approaches, e.g., diffusion cell chambers using skin sections, or cell cultures (Filon et al., 2004; Moser et al., 2001), provide a more efficient way to measure percutaneous absorption of products across the various skin layers. However, there are still some limitations considering the penetration depth of the compounds and the quantification of the precise amount of product that accumulates in each cell layer. In addition, the normal physiological processes of the skin in vivo, which are likely to influence percutaneous penetration of products, such as desqua-

*Correspondence to: Teresa Pinheiro, Laboratório de Feixes de Iões, Instituto Tecnológico e Nuclear, E.N. 10, 2685-953 Sacavém, Portugal. E-mail: murmur@itn.pt

Received 15 May 2006; accepted in revised form 23 October 2006

Contract grant sponsor: SPDV (Portuguese Society of Dermatology and Venereology) Foundation; Contract grant number: SPDV-HM-2002; Contract grant sponsor: European Commission; Contract grant number: EC/QLK4-CT-2002-02678.

DOI 10.1002/jemt.20402

Published online in Wiley InterScience (www.interscience.wiley.com).

mation and sebum secretion cannot be replicated in vitro. It is therefore imperative to develop methodologies enabling the visualization of skin permeability in vivo, providing at least 2D images with quantitative measures of the permeating vehicle, or molecule, which eventually may arrive at very low concentrations in the viable epidermis (Forslind, 2000; Hostynek et al., 2001).

Nuclear microscopy is especially proficient when trace metal quantities are to be determined. It is a technique based on a focused beam of MeV particles, usually protons, generated by a small accelerator that has the capability of imaging the morphology of the tissue and producing the corresponding elemental distribution maps, whether they are major, minor, or trace concentrations (Forslind, 2000; Forslind et al., 1997; Johansson et al., 1995; Pallon et al., 2006). This can be accomplished by the simultaneous use of three different ion beam techniques: Scanning transmission ion microscopy (STIM), Rutherford backscattering spectrometry (RBS), and particle induced X-ray emission (PIXE). STIM is particularly suited to study thin samples (30 μm or less) and is based on the transmission of incident protons (from a 1.5 to 3 MeV proton beam) that have not suffered nuclear backscattering collisions. The energy loss of the transmitted protons is dependent on the density variations of the sample, and by measuring density variations high-resolution images ($\sim$0.5 μm) of samples, morphology can be obtained routinely. Beam spatial resolutions below 100 nm have been reported for particular operating conditions (Watt et al., 2003). This is particularly helpful in the study of tissue morphology and structure since it can identify cell boundaries, being particularly proficient in stratified organs such as the skin. Using PIXE analysis, maps of minor and trace elements can be produced through the detection of characteristic X-rays emitted by the sample elements after the ionization of atomic inner-shells by the incident protons. PIXE is a nondestructive analytic procedure allowing the simultaneous detection of multiple elements (virtually from aluminum to uranium). It has excellent quantitative precision and analytical sensitivity (1–10 μg/g on a dry weight basis) for most of the elements detected. Finally, RBS is based on the energy of protons that are backscattered from atomic nuclei in the sample and provides information on the matrix composition and on the thickness of the sample. The combination of PIXE and RBS data allows quantitative measurements of elemental concentrations, therefore adding information on skin elemental profiles to the above-mentioned outputs. Earlier, Forslind and coworkers (1997) studied human skin physiology using nuclear microscopy, and showed epidermal strata to have discrete variations in elemental concentrations. Moreover, some elemental changes could be correlated with the skin's physiological status, whether normal or diseased (Forslind, 2000), although the accurate visualization of tissue morphological details using transmission images was not fully developed at the time. Development of the proton probe optics enabled a reduction of the beam dimensions and to progressively improve image resolution. By combining morphological images with elemental distributions that are obtained through STIM and PIXE/RBS, respectively, important information can be gathered regarding specific cell environments and tissue structures. These features are of the utmost relevance for understanding the penetration profiles of metals, whether allergenic or not, since the cell layers can be imaged along with concentrations, at each layer or at each cell.

This study presents data on human skin morphology and elemental composition through the simultaneous application of the above-mentioned nuclear microscopy methods. Based on the nuclear microscopy's imaging capability in identifying individual cells and strata, a validation procedure for elemental distributions along the differentiating epidermis of human skin will be presented. This procedure can be used in future studies as a helpful tool on trans-epidermal and -dermal delivery of products. Finally, a review of the available microscopy techniques relevant for the study of skin morphology and physiology will be presented, along with the major benefits and limitations of each technique.

MATERIALS AND METHODS

Materials

Human skin was collected by punch biopsy of 3-mm diameter at lumbar–sacral region, immediately frozen in 2-methylbutane cooled in liquid nitrogen (LN), and kept in the appropriate containers at -80°C or in LN containers until processing. Specimens were supported by mounting medium for microscopy (OCT^{TM} compound), guaranteeing that they would not become fully immersed. Sections of 14-μm thick were cut from the nonimmersed portion of the tissue in a cryostat at -25°C. Sections were allowed to dry inside the cryostat and mounted in specific frames in self-supported mode hold at the edges with Agar^{TM} carbon tape.

The present work is based on a compilation of data from 10 individuals aged 25–66 years (6 women and 4 men), without skin afflictions. The study was performed in accordance with applicable regulatory requirements for ethical and clinical practice. All subjects were informed of the objectives of the study and each was given a consent form. Patient confidentiality was also assured.

Nuclear Microscopy Techniques

The nuclear microscopy techniques used in this study were incorporated into and implemented in our nuclear microprobe set-up. In a nuclear microprobe (NMP), charged particles, most frequently protons or He^{+}, can be focused using electric or magnetic fields. The charged particles are generated in a small accelerator with accelerating voltages typically between 1.5 and 3 MV.

The essential components of the nuclear microprobe constitute a focusing system, a scanning system, an irradiation chamber where several detectors and devices can be connected, and adequate data collection modules, as represented in Figure 1. Samples are usually analyzed in vacuum.

The focusing system contains two sets of slits in addition to the lens system. The first set of slits is called the object from which the system of lenses produces their demagnified image on the sample at the focal plane. The opening of these slits controls the beam transmission/resolution parameters. The second set of slits, the aperture slits, define the beam divergence into the lens

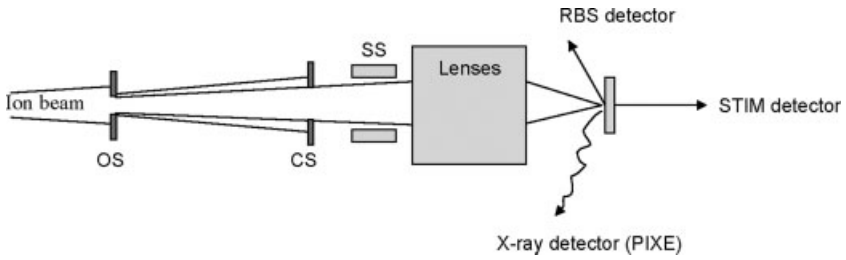

Fig. 1. Schematic of the basic components of a nuclear microprobe focusing system. OS, object slits; CS, collimation slits; SS, scanning system for beam deflection.

system by limiting lens aberrations, such as the spherical aberration. Typical values of 4–8 m for the distance between object and collimation slits and 8–16 cm for the distance between the lens system exit and the image or target plane can be found in the nuclear microprobe set-ups used in this work at CENBG (Moretto, 1996), ITN (Alves et al., 2000), and Lund Institute of Technology (Malmqvist et al., 1993). The final attainable beam's spatial resolution is dependent on several parameters such as accelerator stability, quality of the lens system, mechanical vibrations damping, and thermal stability. Nevertheless, dimensions of 1–3 μm are easily attained on a routine basis for backscattering imaging and ~0.5 μm for transmission imaging. The high spatial resolution of the beam coupled with a scanning range of 1–3 mm improves the imaging capabilities of the system and permits the scanning of a selected region of interest in the sample.

The irradiation chamber can accommodate the placement of a Si(Li) or Ge detector for X-ray detection (PIXE analysis, e.g., minor and trace elements in skin), a Si surface barrier detector for backscattered particles (RBS analysis of matrix constituents, e.g., carbon, nitrogen, and oxygen), a collimated windowless photodiode or a Si surface barrier detector for transmitted particles (STIM analysis of the energy loss of particles across sample), and a Faraday-cup for beam charge measurements. The target holder is mounted on a *x*, *y*, *z* manipulator for positioning the target into the lens focus plane with the help of a microscope.

Detector signals are amplified by a preamplifier and a spectroscopy amplifier. The fast count rate signals are fed into ADCs (analogue to digital converter) with each recorded event assigned to a digital positional coordinate. Thus, electronic components are essential not only for assuring power stability of the lens system, but also for data acquisition and operational control through a computer interface. Data acquisition is made by a multiparameter and a multidetector system that provides several modes of operation to generate bidimensional maps (Elfman et al., 1999). To integrate this information, the computer codes used were either commercially available such as, GeoPIXE II, (Ryan et al., 2005), and OMDAQ (Grime and Dawson, 1995) or the codes were developed in-house by adapting commercial software environments for image processing (Michelet-Habchi et al., 2005). A single map is obtained for the spectral data (X-ray peak area, barrier area, etc.) and for the statistical treatment of the events occurring at each pixel which are then used to produce quantitative elemental maps. Maps can be generated on-line using qualitative information taken from spectra energy intervals, or off-line if all the events were recorded in an "event-by-event" mode. For any given scanned area, spectral information can be extracted from a selected region (regular or irregular in shape) and analyzed separately. Point analysis is also possible either by selecting independent isolated details or specific transects.

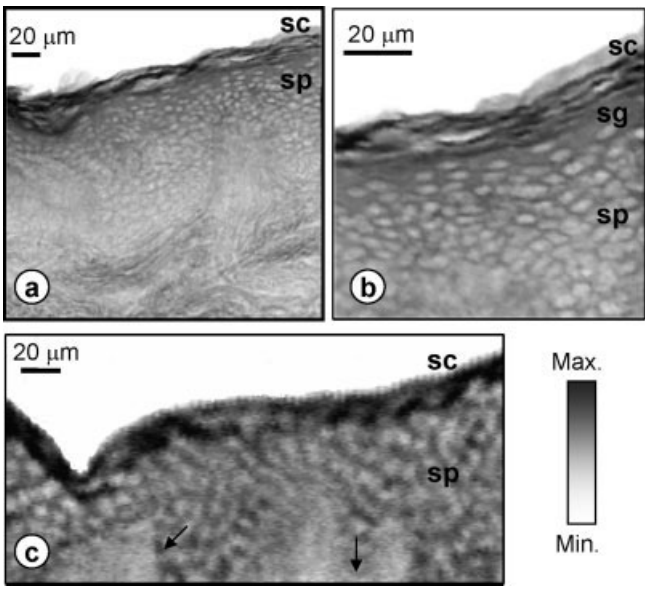

Fig. 2. Human skin density images obtained with high-resolution STIM (**a**), (**b**) general geometry, (**c**) STIM images obtained simultaneously with PIXE and RBS. sc, *stratum corneum*; sg, *stratum granulosum*; sp, *stratum spinosum*; arrows indicate basal layer of epidermis.

RESULTS

Nuclear Microscopy Imaging

High-resolution images of skin sections were obtained with STIM, and the tissue details were easily identified (Figs. 2a and 2b). STIM allowed not only the differentiation of the various cell layers of the skin and therefore the identification of strata, but it also gave further details on a cell to cell level in small scan areas (Fig. 2b). Since STIM is based on the differential energy transmission of the incident particles through the sample, it also enabled the visualization of different density areas providing additional information on skin structure and morphology. This technique can be used in different geometric assemblies as a stand-alone technique or in parallel with other techniques, such as PIXE and RBS (Aguer et al., 2005; Pallon et al., 2004). In the RBS condition, there is a loss in lateral resolution that is compensated for by on-line imaging of mass density. This was helpful in distinguishing tissue

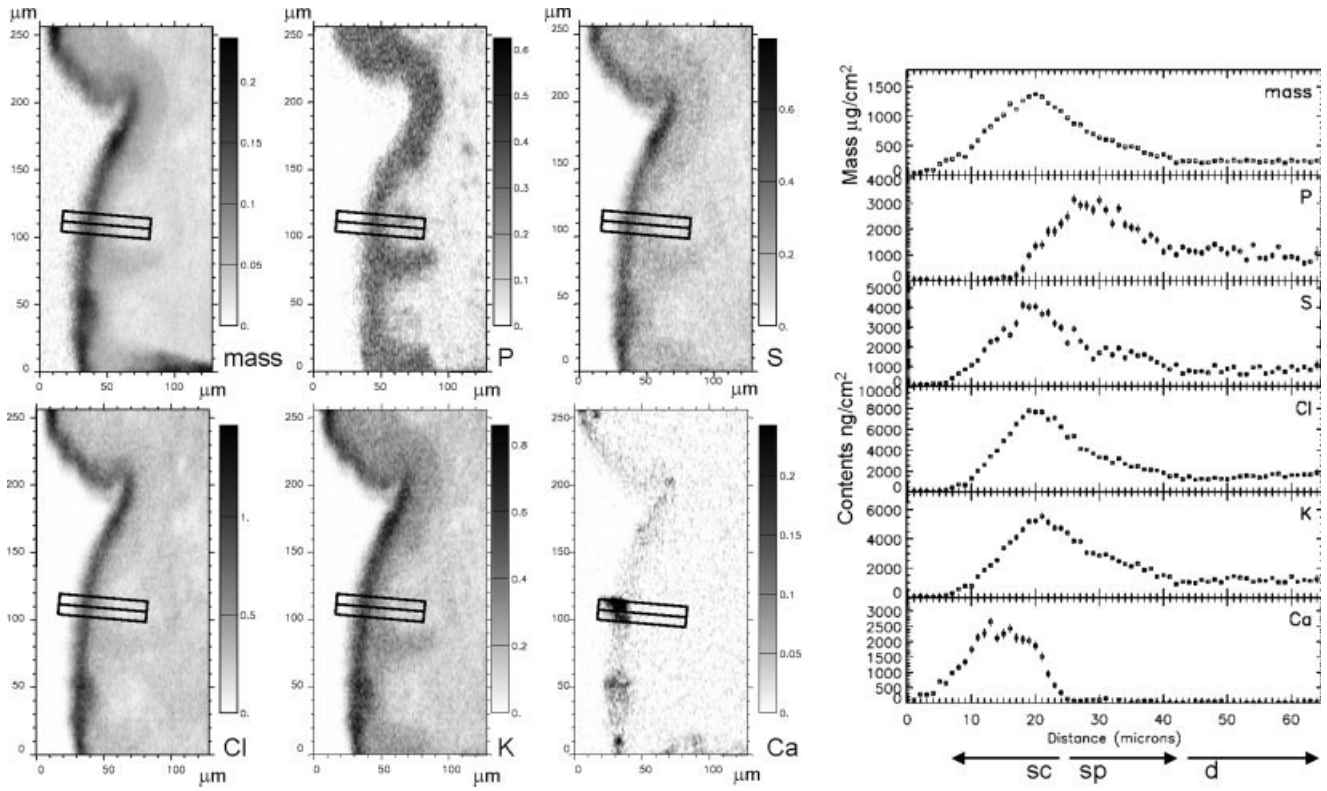

Fig. 3. Quantitative distribution maps (left) and profiles (right) corresponding to the transept indicated in the maps of mass, P, S, Cl, K, and Ca. Gradients from white to black indicate increasing concentrations in maps. sc, *stratum corneum*; sp, *stratum spinosum*; d, dermis.

details, such as *stratum corneum* high density regions, epidermis and dermis (Fig. 2c).

In conjunction with STIM, simultaneous RBS and PIXE analysis produce elemental maps of a given scan area (Fig. 3). When applied to transects, elemental profiles can be obtained or extracted from maps. Both maps and profiles can be fully quantitative, since for each beam position (positional coordinate) the density and thickness of the specimen given by RBS or STIM and the measurement of the impinging number of particles are known. Thus, the concentrations of the various elements can be accurately linked to each skin strata. For healthy human skin, phosphorus (P) and potassium (K) concentrations sharply decreased in the *stratum corneum* (Fig. 3). On the other hand, calcium (Ca) concentrations were remarkably increased in the *stratum corneum* while the iron (Fe) and zinc (Zn) concentrations remained essentially constant in the epidermis (data not shown). At the epidermal–dermal interface, the Fe and Zn concentrations were at least 2-fold higher relative to the values observed in *stratum spinosum* or dermis. Also, a decreasing trend in the Fe contents of dermis and *stratum corneum* were observed (Fe and Zn images and data not shown in Fig. 3). The concentrations of sulfur (S) and chlorine (Cl) were higher in *stratum corneum* when compared to the steady and lower values of *stratum spinosum*. The observed distributions and concentrations agree with previous reported data for human skin (Forslind et al., 1997; Pallon et al., 2006). No significant gender variations were observed in skin elemental concentrations and distribution pattern, although the limited statistical significance in terms of total number of individuals involved in this work has to be taken into account.

Some elements such as Ca and P produced very distinct and characteristic distribution profiles (Fig. 4), showing a clear difference in the concentration at the boundary between the dead cells of the *stratum corneum* and the living cells of the *strata granulosum*, *spinosum*, and *basale*. The highest Ca concentration levels were observed in the *stratum corneum*, sharply decreasing in the *stratum granulosum* and remaining relatively constant along the epidermis and papillary dermis as can be observed in Figure 4. The lowest P concentration level was found in the *stratum corneum* (Fig. 4), increasing in the *stratum granulosum* to concentrations twice as high. The P content progressively increased along the epidermis until the epidermal–dermal junction where it reached a maximum concentration value, and then decreased to concentrations of 4,300 ± 1,800 µg/g in the papillary dermis.

Validation of Skin Layers in Elemental Maps

All elemental profiles obtained from several human skin transects were grouped for each individual element. The distribution of the concentration values was plotted according to the distance from the *stratum corneum*/*stratum granulosum* interface, in 3 µm intervals. The *stratum corneum*/*stratum granulosum* interface was first discriminated through STIM high-resolu-

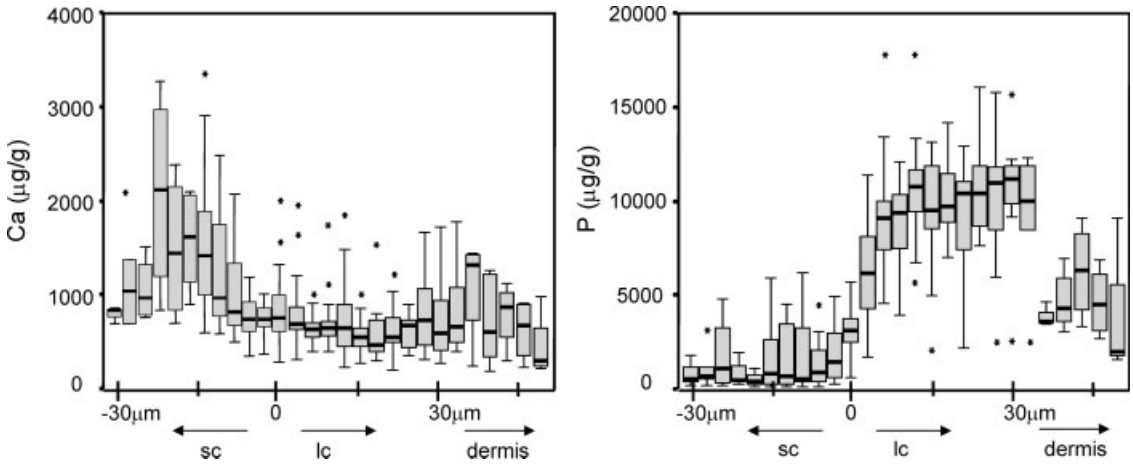

Fig. 4. Distribution of Ca and P levels with distance from the base of the *stratum corneum*/living cells interface (3 µm intervals). Box plots showing median; box length: interquartile range; bars: 1.5 box length; and outliers (*): >1.5 box length (sc, *stratum corneum*; lc, living cells).

tion images. From the characteristic elemental distributions observed, for P, Cl, K, and Ca, the interval of concentrations at the *stratum corneum–granulosum* interface was estimated using a logistic fit procedure. Standard deviations for each concentration value were used as weighting for the function parameters estimation (i.e., upper and lower asymptotes, half height and rate of the curve, and respective errors).

The results obtained for P distribution were found to constitute the best estimate for strata characterization, as exemplified in Figure 5. In fact, the half height of the fitted curve set the interface between the *stratum corneum* and the first line of living cells (*stratum granulosum*) as 2.20 ± 0.02 µm, a very good approximation to the coordinate value extracted from STIM images (considered as zero in the graph). At this interface, the P concentration calculated from the function fit was 5,110 µg/g. The upper and lower asymptote values provided an estimation of average concentration levels for *stratum spinosum* and *stratum corneum*, respectively.

The method described earlier can be applied to skin exposed to formulations containing a permeation molecule with a metal ion or dispersed nanoparticles. As exemplified in Figure 6, the distribution, coverage, and permeation of nanoparticles of titanium (Ti), used as physical filters of UV radiation in sunscreens, along skin can be studied. The image of a human skin longitudinal section shows a patchy distribution of Ti in the surrounding of the opening of an air follicle onto the skin surface. The Ti profile showed a maximum for the *stratum corneum* outer layers, quickly decaying to concentration levels within the minimum detectable concentration range (Pallon et al., 2005) and continuing without significant variations once in the living cell layers. P contents remained low along all the *stratum corneum* length increasing beyond the *stratum granulosum*. Therefore, both the elemental maps and the diffusion profiles can be linked with STIM images and P (or Ca, as shown earlier) profiles can be used to determine and validate the depth of penetration and skin strata involved. Furthermore, the cell layers interacting with the permeation molecule and quantitative diffusion profiles according to dose can in due course be established.

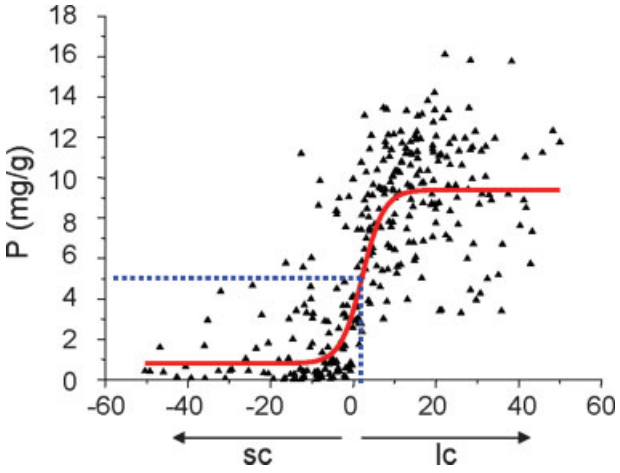

Fig. 5. Elemental profile of P according to distance (in µm) from the *stratum corneum*/*stratum granulosum* interface (zero in the graph) to *stratum corneum* (sc) and to living cells of epidermis. The logistical fit gives an adjustment of 2.2 ± 0.02 µm to the initial zero value (dashed line). Low P concentration: 791 ± 11 µg/g; high P concentration: 9,395 ± 13 µg/g; *P* values at 1/2 height: 5,110 µg/g; R^2 = 0.74. [Color figure can be viewed in the online issue, which is available at www.interscience.wiley.com.]

DISCUSSION

Nuclear microscopy can provide useful and complementary information compared with that obtained from conventional histological and histochemical methods and other microanalytical microscopes. In this work, it was demonstrated that the skin morphology at the cell level is easily recognized through relatively high-resolution images obtained with STIM. In addition, the elemental maps and distributions acquired are fully quantitative with a good sensitivity at the microgram per gram level (on a dry weight basis). A typical analysis of a sample area of ~0.04 mm^2 can be

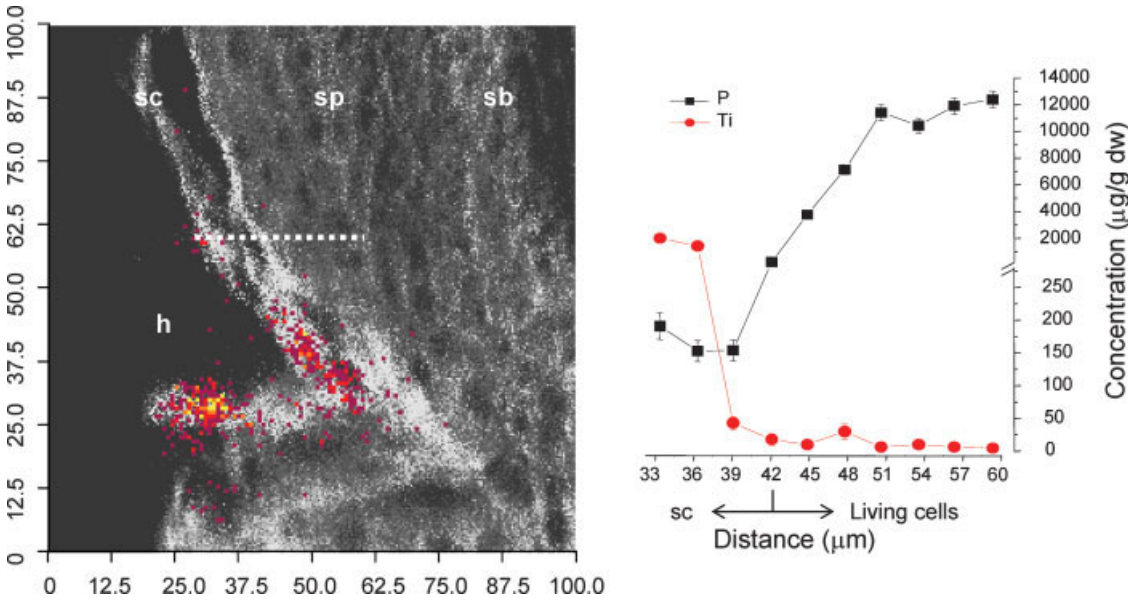

Fig. 6. Human skin image covering a hair follicle opening (h) onto the skin surface where a patchy distribution of titanium (white/color) can be observed. The titanium image was overlapped with the STIM density image (from low density—black, to high density—white). In the graph, the concentrations of Ti and P along skin, for the transept indicated by the dashed line on the map, are plotted for 3 μm distance intervals. The titanium permeation is limited to *stratum corneum* (sc) outer layers. sp, *stratum spinosum*; sb, *stratum basale*. [Color figure can be viewed in the online issue, which is available at www.interscience.wiley.com.]

easily achieved in 2 h, even for elements in low concentration levels. Both the elemental maps and the diffusion profiles of a permeating molecule can be correctly correlated with STIM images, enabling the accurate determination of the concentrations at each skin strata. In addition, diffusion profiles can be determined quantitatively and the effect of each dose level can be established in vivo.

Forslind and coworkers have called attention to the potential of nuclear microscopy by studying the physiology of human skin in health and in pathological conditions, as elemental profiles could be obtained and linked to skin strata and therefore to the differentiation of keratinocytes (Forslind, 2000; Forslind et al., 1997). The elemental concentrations in skin observed in this work fully agree with previous published data, where the elemental variations within the epidermis, especially P, Cl, and Ca, were associated with specific physiological functions of skin and keratinocyte differentiation. In the present work, the simultaneous use of STIM and PIXE made it possible to image and identify skin strata, directly associating them to elemental distributions, which is crucial in permeation studies. In addition, the discrete variations in the concentration profiles of P, Cl, K, and Ca, among other elements, with epidermis depth can be used to accurately identify cell strata, enabling further studies of dermatological medical condition where the metabolism of essential elements are involved. Alterations in these profiles were used to characterize skin condition and pathology as electrolyte imbalances could be related to proliferation and upregulation of inflammatory mediators (Forslind, 2000; Pallon et al., 2006).

The most relevant feature of nuclear microscopy is the ability of inspecting tissues and cells, preserved as close as possible to their in vivo condition, while providing good image resolution and contrast, and fully quantitative data at the microgram per gram levels. This is particularly useful in skin permeability studies, since by avoiding pretreatment steps in tissue preparation, such as chemical fixation, the tissue structure and elemental distribution integrity can be maintained. Nonetheless, the diffusion of permeation molecules across skin is only traceable if the target compound contains a metal ion or an element possible to be measured by PIXE. Also, the identification of chemical species or compounds is not possible, as only atoms are detected. These aspects constitute the major limitations of nuclear microscopy analysis. The simultaneous use of STIM, PIXE, and RBS techniques provided important information about the distribution of elements, the density profile, and the morphological arrangement of the different cell layers of the skin. By correlating image information obtained through STIM with quantitative elemental maps from PIXE and RBS, elemental distribution patterns can be accurately associated with tissue morphology. As time-dependent information is linked to spectra acquisition and imaging, tissue damage, which eventually occurs during irradiation, can also be estimated by assessing intermediate stages of analysis from the initial to the final stage. Although in terms of lateral resolution nuclear microscopy cannot compete with other microanalytical microscopies, e.g., electron microscopy, as technology evolves, system resolutions are being forced down to the 40 nm or less and 3D capabilities (tomography) can also be added, which constitutes an outstanding benefit in cell morphology and cell physiology studies (Dymnikov et al., 2005; Ross et al., 2005; Schwertner et al., 2006).

When studying the physiology and morphology of the skin, and in particular the permeation of chemicals and/or metal ions, it is important to have a detailed

characterization of cell layers. Different microscopy techniques, based on light, electrons, or other sources of radiation, could also provide relevant morphological information and quantitative data on elemental distributions that can be useful for studying the permeation of a chemical through skin.

Transmission electron microscopy (TEM) or scanning electron microscopy (SEM) with associated X-ray microanalysis offers excellent resolution of ultrastructure details and the use of cryosections is also possible, to guarantee tissue integrity in an in vivo condition. Although methodologies can be adapted to produce better detection limits at the expense of resolution, the quantification of a permeating chemical is demanding, as it often requires the determination of trace quantities. The detection limits for a wide range of elements obtained in ultrathin and semithin section analysis are of the order of several hundreds of microgram per gram making trace elemental analysis unfeasible (Forslind et al., 1997; Pallon et al., 2006; Pechtold et al., 2001). Even when carrying out elemental analysis in thicker cryosections ($\geq$15 μm) and dramatically limiting spatial resolution to a few micrometers (Kozlova and Roomans, 2003), the improvement in detection limits is not sufficient. Nevertheless, the technique is proficient in studying electrolyte distribution in tissues in vivo such as, Na, Cl, K, and Ca, or Fe accumulation in organs or cells, which are often in concentrations of the order of milligram per gram (Akar et al., 2003; Kozlova and Roomans, 2003; Rohrbach et al., 2005; Vanthanouvong et al., 2003).

Synchrotron radiation as a bright source of infrared or hard X-rays photons has been exploited in microscopy for the study of tissues, individual cells, and for functional group imaging. By using infrared spectroscopy, X-ray fluorescence, and absorption edge spectrometries, excellent detection limits for specific compounds, metals and metal species, respectively, are possible (Dumas and Miller, 2003; Golosio et al., 2003; Harris et al., 2005). These techniques can be combined in biological research and would constitute an outstanding set of tools, although assessing fully quantitative results is still a challenging task and resolutions achieved in elemental imaging are so far limited to a few micrometer. Soft X-ray microscopy and X-ray diffraction microscopy are emerging techniques, based on sample irradiation by a coherent beam of soft X-rays. This approach makes it possible to image hydrated or frozen-hydrated biological specimens and cells at 10-nm resolution in two or three dimensions (Johansson et al., 2004; Shapiro et al., 2005). So far, elemental analysis is modest as beam energies are limited to $\sim$1 keV.

Light, electron, laser, and X-ray microscopy are important techniques for the analysis of cellular structure physiology and function of biological tissues. In spite of their many advantages in various applications, they require an extensive chemical treatment of the tissue before examination (Haftek et al., 1998). Furthermore, the quantitative determination of metals in in-vivo condition and its eventual diffusion across skin layers can be a difficult task to achieve, as metals are often weakly bound to organic structures and therefore easily mobilized (Filon et al., 2004; Hostynek, 2003). Conventional histological or histochemical methods based on light microscopy allow direct examination of viable or fixed cells and tissues using stains or fluorescent probes or radioactive tracers. Though it is possible to follow the permeation of a molecule using these methodologies, chemical fixation may induce delocalization or a partial loss of the metals from the tissue. In addition, the out-of-focus condition due to overlapping tissue structures cannot be totally circumvented even with modern image contrast-enhancing software. Confocal laser scanning microscopy provides semiquantitative high-resolution images ($<$1 μm). It can prevent some of the imaging artifacts since it avoids fixation and sectioning, but it is drastically limited by the range of lasers for which efficient fluorophore excitation can be achieved (Alvarez-Román et al., 2004). Although many fluorescent probes are available commercially to assess skin physiology, the existence of an adequate fluorophore for molecular analysis can be a difficult prerequisite to fulfill (Grams and Bouwstra, 2002). In theory, a depth profile of the permeant can be achieved, though some difficulties need to be overcome in what concerns the relationship between the signal obtained and an absolute concentration. Laser illumination of viable tissue can also be destructive both for cells and for the fluorophore resulting in photobleaching. Nevertheless, the technique offers the ability to assess endogenous biological molecules (aminoacids, peptides, proteins, phospholipids, enzymes, coenzymes, etc.). Mechanistic studies addressing the preferred penetration pathways following the use of different delivery processes are also possible to conduct using this technique.

In summary, for the particular case of skin permeation studies, nuclear microscopy shows appealing advantages, as it enables in vivo examination of the metal plus carrier permeation, its imaging, and a quick and accurate evaluation of its depth of penetration. The analysis is relatively fast and costs are similar to those of an electron microprobe. Although the installation of a NMP system is restricted to laboratories with small particle accelerator facilities, more than 100 laboratories spread worldwide have nuclear microscopy capabilities. An increasing number of set-ups have been upgraded to submicrometer resolution with tomographic imaging capabilities, which is a clear advantage over conventional microscopies. The fast development of detectors and instrumentation for beam focusing, as well as for producing brighter sources of radiation capable of exciting atomic inner-shells will undoubtedly overcome the present deficiencies and will a complementary method for biological imaging.

Despite the advantages and disadvantages that can be associated with these techniques the quantitative determination of metals in an in vivo condition with its eventual diffusion across skin layers has been a difficult undertaking. Metal oxides are widely spread in modern hygiene products with no restrictions to topical use by consumers. Metals play a vital role in human physiology although the mechanisms by which they penetrate through skin or induce skin responses are far from being understood.

REFERENCES

Aguer P, Alves LC, Barberet Ph, Gontier E, Incerti S, Michelet-Habchi C, Kertész Zs, Kiss AZ, Moretto P, Pallon J, Pinheiro T, Surlève-Bazeille J-E, Szikszai Z, Veríssimo A, Ynsa MD. 2005. Skin morphology and layer identification using different STIM geometries. Nucl Instrum Methods B 231:292–299.

Akar JG, Everett TH, Ho R, Craft J, Haines DE, Somlyo AP, Somlyo AV. 2003. Intracellular chloride accumulation and subcellular elemental distribution during atrial fibrillation. Circulation 107:1810–1815.

Alvarez-Román R, Naik A, Kalia YN, Fessi H, Guy RH. 2004. Visualization of skin penetration using confocal laser scanning microscopy. Eur J Pharm Biopharm 58:301–316.

Alves LC, Breese MBH, Alves E, Paúl A, da Silva MR, Soares JC. 2000. Micron-scale analysis of SiC/SiC_f composites using the new Lisbon nuclear microprobe. Nucl Instrum Methods B 161–163:334–338.

Barry BW. 2001. Is transdermal drug delivery research still important today? Drug Discov Today 6:967–971.

Dumas P, Miller L. 2003. The use of synchrotron infrared microspectroscopy in biological and biomedical investigations. Vib Spectrosc 32:3–21.

Dymnikov AD, Glass GA, Rout B. 2005. Zoom quadrupole focusing systems producing an image of an object. Nucl Instrum Methods B 241:402–408.

Elfman M, Kristiansson P, Malmqvist K, Pallon J. 1999. The layout and performance of the Lund nuclear microprobe trigger and data acquisition system. Nucl Instrum Methods B 158:141–145.

Filon FL, Maina G, Adami G, Venier M, Coceani N, Bussani R, Massiccio M, Barbieri P, Spinelli P. 2004. In vitro percutaneous absorption of cobalt. Int Arch Occup Environ Health 77:85–89.

Fluhr JW, Akengin A, Bornkessel A, Fuchs S, Praessler J, Norgauer J, Grieshaber R, Kleesz P, Elsner P. 2005. Additive impairment of the barrier function by mechanical irritation, occlusion and sodium lauryl sulphate in vivo. Br J Dermatol 153:125–131.

Forslind B. 2000. The skin barrier: Analysis of physiologically important elements and trace elements. Acta Derm Veneorol 208(Suppl):46–52.

Forslind B, Lindberg M, Roomans GM, Pallon J, Werner-Linde Y. 1997. Aspects of the physiology of human skin: Studies using particle probe analysis. Microsc Res Tech 38:373–386.

Golosio B, Simionovici A, Somogyi A, Lemelle L, Chukalina M, Brunetti A. 2003. Internal elemental microanalysis combining X-ray fluorescence, compton and transmission tomography. J Appl Phys 94: 145–156.

Grams YY, Bouwstra JA. 2002. A new method to determine the distribution of a fluorophore in scalp skin with focus on hair follicles. Pharm Res 19:350–354.

Grime GW, Dawson M. 1995. Recent developments in data acquisition and processing on the Oxford scanning proton microprobe. Nucl Instrum Methods B 104:107–113.

Hadgraft J. 2004. Skin deep. Eur J Pharm Biopharm 58:291–294.

Haftek M, Teillon M-H, Schmitt D. 1998. Stratum corneum, corneodesmosomes and ex vivo percutaneous penetration. Microsc Res Tech 43:242–249.

Harris HH, Levina A, Dillon CT, Mulyani I, Lai B, Cai Z, Lay PA. 2005. Time-dependent uptake, distribution and biotransformation of chromium(VI) in individual and bulk human lung cells: Application of synchrotron radiation techniques. J Biol Inorg Chem 10: 105–118.

Hostynek JJ. 2003. Factors determining percutaneous metal absorption. Food Chem Toxicol 41:327–345.

Hostynek JJ, Dreher F, Pelosi A, Anigbogu A, Maibach HI. 2001. Human stratum corneum penetration by nickel. In vivo study of depth distribution after occlusive application of the metal powder. Acta Derm Venereol 212(Suppl):5–10.

Johansson GA, Khanna SM, Nair A, Mannström P, Denbeaux G, Ulfendahl M. 2004. Exploring the use of soft X-ray microscopy for imaging subcellular structures of the inner ear. J Microsc 215:203–212.

Johansson SAE, Campbell JL, Malmqvist KG. 1995. Particle induced X-ray emission spectrometry. New York: Wiley. 451p.

Kozlova I, Roomans GM. 2003. Preservation of pancreas tissue during cold storage assessed by X-ray microanalysis. Am J Transplant 3: 697–707.

Löffer H, Dreher F, Maibach HI. 2004. Tape stripping procedure: Influence of anatomic site, application pressure, duration and removal. ESCD Abstracts 2004. Contact Dermatitis 50:135.

Malmqvist KG, Hyltén G, Hult M, HÅkansson K, Knox JM, Larsson NP-O, Nilsson C, Pallon J, Schofield R, Swietlicki E, Tapper UAS, Changyi Y. 1993. Dedicated accelerator and microprobe line. Nucl Instrum Methods B 77:3–7.

Michelet-Habchi C, Incerti S, Aguer P, Barberet Ph, Gontier E, Grente K, Moretto Ph, Nguyen DT, Pouthier A, Pouthier T, Rebillat F, Smith RW. 2005. TomoRebuild: A new data reduction software package for scanning transmission ion microscopy tomography. Nucl Instrum Methods B 231:142–148.

Moretto Ph. 1996. Nuclear microprobe: A microanalytical technique. Cell Mol Biol (Noisy-le-grand) 42:1–16.

Moser K, Kriwet K, Naik A, Kalia YN, Guy RH. 2001. Passive skin penetration enhancement and its quantification in vitro. Eur J Pharm Biopharm 52:103–112.

Nielsen GD, Nielsen JB, Andersen KE, Grandjean P. 2000. Effects of industrial detergents on the barrier function of human skin. Int J Occup Environ Health 6:138–142.

Pallon J, Auzelyte V, Elfman M, Garmer M, Kristiansson P, Malmqvist K, Nilsson C, Shariff A, Wegdén M. 2004. An off-axis STIM procedure for precise mass determination and imaging. Nucl Instrum Methods B 219/220:988–993.

Pallon J, Garmer M, Auzelyte V, Elfman M, Kristiansson P, Malmqvist K, Nilsson N, Shariff A, Wegdén M. 2005. Optimization of PIXE-sensitivity for detection of Ti in thin human skin sections. Nucl Instrum Methods B 231:274–279.

Pallon J, Forslind B, Lindberg M. 2006. Particle probes and skin physiology. In: Lodén M, Maibach HL, editor. Dry skin and mosturizers: Chemistry and function, 2nd ed. Boca Raton, FL: CRC Press. pp. 44–61.

Pechtold LA, Boddé HE, Junginger HE, Koerten HK, Bouwstra JA. 2001. X-ray microanalysis of cryopreserved human skin to study the effect of iontophoresis on percutaneous ion transport. Pharm Res 18:1012–1017.

Rohrbach P, Friedrich O, Hentschel J, Plattner H, Fink RHA, Lanzer M. 2005. Quantitative calcium measurements in subcellular compartments of *Plasmodium falciparum*-infected erythrocytes. J Biol Chem 280:27960–27969.

Ross GJ, Bigelow AW, Randers-Pehrson G, Peng CC, Brenner DJ. 2005. Phase-based cell imaging techniques for microbeam irradiations. Nucl Instrum Methods B 241:387–391.

Ryan CG, Etschmann BE, Cousens DR. 2005. GeoPIXE II, CSIRO Exploration and Mining, Bayview Road, Clayton VIC 3168, Australia. Available from http://nmp.csiro.au/GeoPIXE.html.

Schwertner M, Sakellariou A, Reinert T, Butz T. 2006. Scanning transmission ion micro-tomography (STIM-T) of biological specimens. Ultramicroscopy 106:574–581.

Shapiro D, Thibault P, Beetz T, Elser V, Howells M, Jacobsen C, Kirz J, Lima E, Miao H, Neiman AM, Sayre D. 2005. Biological imaging by X-ray diffraction microscopy. Proc Natl Acad Sci 102:15343–15346.

Thomas BJ, Finnin BC. 2004. The transdermal revolution. Drug Discov Today 9:697–703.

Tsuji JS, Maynard AD, Howard PC, James JT, Lam C, Warheit DB, Santamaria AB. 2006. Research strategies for safety evaluation of nanomaterials. IV. Risk assessment of nanoparticles. Toxicol Sci 89:42–50.

Van der Molen RG, Spies F, van't Noordende JM, Boelsma E, Mommaas AM, Koerten HK. 1997. Tape stripping of human stratum corneum yields cell layers that originate from various depths because of furrows in the skin. Arch Dermatol Res 289:514–518.

Vanthanouvong V, Hogman M, Roomans GM. 2003. In vitro and in situ experimental model for X-ray microanalysis of intestinal epithelium. Microsc Res Tech 62:211–214.

Watt F, van Kan JA, Rajta I, Bettiol AA, Choo TF, Breese MBH, Osipowicz T. 2003. The National University of Singapore high energy ion nano-probe facility: Performance tests. Nucl Instrum Methods B 210:14–20.